TELKOMNIKA, Vol. 11, No. 10, October 2013, pp. 6158 ~ 6165
ISSN: 2302-4046

Car Information Bus Image Restoration Using Multi-wavelet Transform Algorithm

Zhuangwen Wu*, Liangrong Zhu, Hailei Ren
Zhejiang Industry Polytechnic College
Jinghu New District, Shaoxing, Zhejiang Province, P.R.China, Ph./Fax: +86-575-88009255
*Corresponding author, e-mail: patiant@126.com

Abstract

Car reverse image is transmitted by information bus. Because of the bad electromagnetic environment of the engine compartment, car's information bus sometime will be blocked or not real-time, which can lead to the uncertainty of information transmission, and will cause the risks of security and reliability of the transmitted network. A GHM multi-wavelet is adopted by this paper to restore the interference car reverse image. After balanced processing the GHM multi-wavelet, constant module blind equalization algorithm based on balanced orthogonal multi-wavelet transform (MWTCMA) is used in this paper. Compared with the constant module blind equalization algorithm (CMA) and wavelet transform constant module blind equalization algorithm (WTCMA), results show that MWTCMA can eliminate the multi-wavelet pre-filtering process through multi-wavelet transform on input signal, and improve the convergence speed. The calculation error of MWTCMA is also smaller than the other two methods.

Keywords: *MWTCMA, Car Information Bus, Image Restoration*

1. Introduction

Applied on network protocol, some entertainment information of modern car is often transmitted by information bus with its differential transmission technology, communication non-destructive arbitration and scheduling priority competition mechanism [1]. Because of the bad electromagnetic environment of the engine compartment, car's information bus sometime will be blocked or not real-time, which can lead to the uncertainty of information transmission. Thus it will cause the risks of security and reliability of the transmitted network [2].

In order to solve this problem, many scholars begin to study on blind equalization technology, which was first applied by Sato to multi-amplitude modulation data transmission restoration from a balanced image. Miucic R. and YAN Nan-ming presented the presence of inter-symbol interference channels, using multilayer neural network structure based on decision feedback equalizer [3-4]. Yun Seok Choi and Kyun Hyon Tchah used two-order and four-order-moment method, which is not only applicable to the non-Gaussian data transmission, but also suitable for Gauss data transmission [5]. And then study on the safety and reliability of the car network transmission scheduling appeared. Yu Linan and Shin studied the fixed priority scheduling and real-time analysis [6-7]. Goossens B and Ho S Hong applied neural network for equalization and decoding [8-9]. Hong SH and Kim WH discussed that the neural network can be used to simultaneously complete equalization and decoding scheme based on adaptive artificial neural network equalizer [10]. Niu Dejiao, Pascal Bianchi, et al. researched on scheduling algorithms united with controlling and communication [11-12]. Then Nolte T and Nolin M studied on blind equalization combining constant modulus algorithm with Gauss algorithm [13]. Afonso MV applied neural network on blind equalization [14]. Then multilayer neural network structure was applied to digital communication adaptive equalization by Johnson BR [15]. Now, the combination algorithm presented by Fowler JE can identify channels according to the channel change equalizer structure by different tracking and acquisition of adaptive algorithm [16].

Although these programs are relatively simple and have a small amount of computation, the convergence rate is slow, which can not meet modern car information transmission requirements on large data, long distance and high transmission speed. With the continuous

Received March 18, 2013; Revised July 14, 2013; Accepted July 24, 2013

improvement of modern car on power, comfort, and safety, the quality of car information bus scheduling is also need continuously improve [17].

Because of symmetry, orthogonality and finite supporting, GHM multi-wavelet are adopted by this paper to restore the interference car reverse image, transmitted by information bus, through MWTCMA. Compared with the CMA and WTCMA [14], MWTCMA can eliminate the multi-wavelet pre-filtering process through multi-wavelet transform on the input signal, and improve the convergence speed. The calculation error of MWTCMA is also smaller than the other two methods.

2. Mathematical Model

The blind equalizer based on orthogonal multi-wavelet transform is constructed as shown in Figure 1.

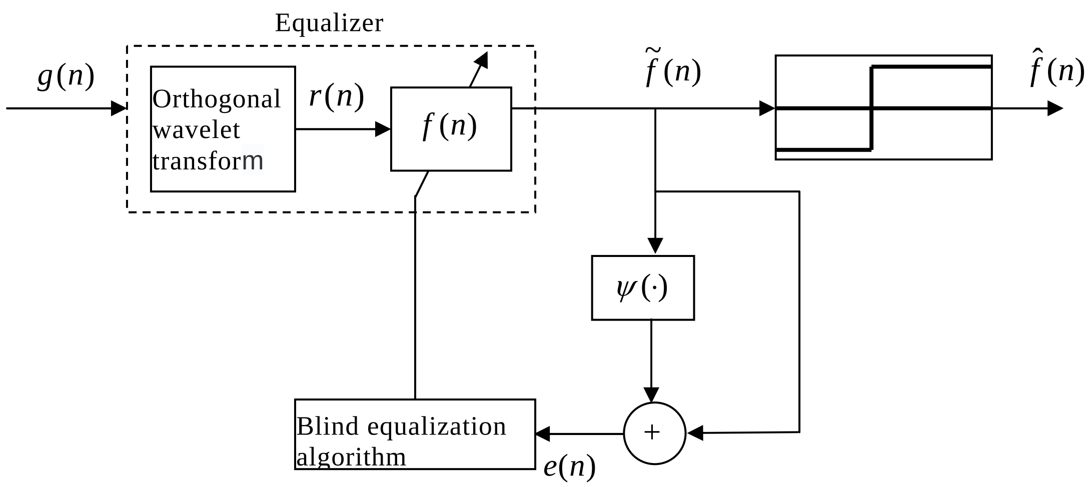

Figure 1. Blind equalization algorithm based on orthogonal multi-wavelet transform

In Figure 1, $g(n)$ is the equalizer input signal, and the output signal is $\tilde{f}(n)$. The response of the equalizer $f(n)$ at time n is $f_i(n)$, (where $i = 0,1,\ldots,N-1$, *N* is the order number of the equalizer), $\psi(\cdot)$ is the mean square error (MSE) determination unit. The maximum scale of multi-wavelet transform is $J \in \boldsymbol{Z}$, the maximum translation under scale j is $k_j = N/2^j$. Due to the impulse response of the equalizer $f_i(n)$ is limited, hence it can be defined by multi-wavelet as:

$$f_i(n) = \sum_{l=1}^{r}\sum_{j=1}^{J}\sum_{k=0}^{k_j-1} w_{j,k}^{l}(n)\psi_{j,k}^{l}(i) + \sum_{l=1}^{r}\sum_{k=0}^{k_j-1} v_{J,k}^{l}(n)\varphi_{J,k}^{l}(i) \tag{1}$$

where $\varphi_{J,k}^{l}(i)$ is the l-th scaling function when the translation is k and the scale parameter is j, and $\psi_{j,k}^{l}(i)$ is the l-th wavelet-base function when the translation is k and the scale parameter is j.

When scaling function and wavelet function are selected, the characteristics of the equalizer can be decided by $w_{j,k}^{l}(n)$ and $v_{J,k}^{l}(n)$. And the equalizer output signal $\tilde{f}(n)$ can be expressed as follows:

$$\tilde{f}(n)=\sum_{i=0}^{N-1} f_i(n)g(n-i)=\sum_{l=1}^{r}[\sum_{j=1}^{l}\sum_{k=0}^{k_j-1} w_{j,k}^{l}(n)r_{j,k}^{w,l}(n)+\sum_{k=0}^{k_j-1} v_{J,k}^{l}(n)r_{J,k}^{v,l}(n)] \quad (2)$$

where $r_{j,k}^{w,l}(n)=\sum_{i=0}^{N-1}\psi_{j,k}^{l}(n)g(n-i)$, is the l-th wavelet-based function convoluted output of the input signal $g(n)$ when the translation is k and the scale parameter is j. $r_{J,k}^{v,l}(n)=\sum_{i=0}^{N-1}\varphi_{J,k}^{l}(n)g(n-i)$, is the l-th wavelet-based function convoluted output of the input signal $g(n)$ when the translation is k and the scale parameter is J.

So, Eq. (2) is the discrete orthogonal wavelet transform of the input signal $g(n)$.

3. Research Method

3.1. Orthogonal Multi-wavelet Transform Matrix

The chosen wavelet should be avoided generating new errors when it's reconstructed or truncated. And it also should have some good characteristics such as better approximation, less calculation, and no overlap in any scale and so on. According to the literature [18], GHM multi-wavelet, which can meet the orthogonality, short supporting, symmetry, two-order vanish moment and other requirements well, is used in this paper. GHM multi-wavelet equalizer is constructed following.

The GHM multi-wavelet can be one-order balanced by using orthogonal unitary matrix $\boldsymbol{U}=\frac{1}{\sqrt{2}}\begin{bmatrix}1 & -1\\ 1 & 1\end{bmatrix}$. After Balancing, the new high-pass filter can be expressed as $\boldsymbol{G}(\omega)=\boldsymbol{G}(\omega)\boldsymbol{U}$, and the new low-pass filter can be expressed as $\boldsymbol{H}(\omega)=\boldsymbol{U}^T\boldsymbol{H}(\omega)\boldsymbol{U}$.

Now, the balanced multi-wavelet Mallat decomposition can be done. Selecting a discrete signal $x=[x_0,x_1,...,x_{m-1}]^{\mathrm{T}}$, ($m\in\mathbf{Z}$), the blocked matrix $\boldsymbol{P}_j$ and $\boldsymbol{Q}_j$ can be defined as [15]:

$$\boldsymbol{P}_j=\begin{bmatrix}\boldsymbol{H}_0 & \boldsymbol{H}_1 & \boldsymbol{H}_2 & ... & 0 & ... & 0\\ 0 & 0 & \boldsymbol{H}_0 & \boldsymbol{H}_1 & \boldsymbol{H}_2 & 0 & ...\\ 0 & ... & & & ... & 0 & ...\\ 0 & 0 & 0 & 0 & \boldsymbol{H}_0 & \boldsymbol{H}_1 & ...\end{bmatrix} \quad (3)$$

where $j=1\sim J$, $l=m/2^{j-1}$, $J,l\in\boldsymbol{Z}$, The definition of matrix $\boldsymbol{Q}_j$ is similar to $\boldsymbol{P}_j$ as $\boldsymbol{H}_i$ replaced by $\boldsymbol{G}_i$ in the matrix. So we can get [19]:

$$\begin{cases} v_j=\boldsymbol{P}_j\boldsymbol{P}_{j-1}...\boldsymbol{P}_1 x\\ w_j=\boldsymbol{Q}_j\boldsymbol{P}_{j-1}...\boldsymbol{P}_1 x\end{cases} \quad (4)$$

where $\boldsymbol{Q}_j$ is the balanced matrix consisted by multiple high-pass filters, v_j and w_j is the low-pass and high-pass coefficient of the input signal x after j-th layer decomposition respectively. The Mallat decomposition of v_j and w_j is shown in Figure 2.

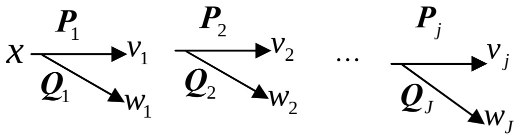

Figure 2. Mallat decomposition of v_j and w_j

Suppose that $\boldsymbol{T}=[\boldsymbol{Q}_1,\boldsymbol{Q}_2\boldsymbol{P}_1,\boldsymbol{Q}_2\boldsymbol{P}_1\boldsymbol{P}_0,...,\boldsymbol{Q}_J\boldsymbol{P}_{J-1},...,\boldsymbol{P}_2\boldsymbol{P}_1,\boldsymbol{P}_J\boldsymbol{P}_{J-1},...\boldsymbol{P}_2\boldsymbol{P}_1]$, which is a balanced orthogonal multi-wavelet transform matrix, we can balanced transform any chosen multi-wavelet by using ***T*** [15].

3.2. Algorithm Description

Suppose the input signal $\boldsymbol{g}(n)=[g(n),g(n-1),...,g(n-N+1)]^{\mathrm{T}}$, the balanced orthogonal multi-wavelet transform signal $\boldsymbol{r}(n)=[r(n),r(n-1),...,r(n-N+1)]^{\mathrm{T}}$. According to the minimum MSE criterion, MWTCMA is:

$$\begin{cases}\mathbf{r}(n)=\mathbf{T}\mathbf{g}(n)\\ \tilde{\mathbf{f}}(n)=\mathbf{f}(n)\overleftarrow{\mathbf{r}}(n)\\ e(n)=\mathbf{R}_2-|\tilde{f}(n)|^2\\ \mathbf{f}(n+1)=\mathbf{f}(n)+\lambda\mathbf{R}^{-1}(n)e(n)\mathbf{r}(n)\overset{*}{\tilde{\tilde{f}}}(n)\\ \mathbf{R}_2=E(|y(n)|^4/E(|y(n)|^2)\end{cases} \tag{5}$$

$$\sigma^2{}_{J,k,m}(n+1)=\beta\sigma^2_{J,k,m}(n)+(1-\beta)|r^m_{j,k}(n)|^2 \tag{6}$$

where $\boldsymbol{r}(n)$ is the transformed signal of the equalizer input signal $\boldsymbol{g}(n)$ by the matrix $\boldsymbol{T}$, λ is the iteration step, and $\overset{*}{\tilde{\tilde{f}}}(n)$ is the conjugate of $\tilde{f}(n)$. And $\mathbf{R}^{-1}(n)=\mathrm{diag}[\sigma_{J,k,0}(n),\sigma^2{}_{J,k,1}(n),-$

$...,\sigma^2{}_{J,k,m}(n),\sigma^2{}_{J+1,k,0}(n),...,\sigma^2{}_{J,k,m}(n)]$, is a diagonal matrix constituted by normalized energy. $r^m_{j,k}(n)$ is the m-th-dimension multi-wavelet coefficients when the translation is k and the scale parameter is j, i.e. the elements of the matrix $\boldsymbol{r}(n)$ of Eq. (5), and β is the iterative coefficient. So MWTCMA can be described by Eq. (5) and Eq. (6). In this algorithm, the multi-wavelet transformed signal, normalized in the frequency domain, also makes the convergence further accelerated.

4. Simulation

The car reverse image, transmitted by information bus, is PAL/NTSC format, whose display distance is less than 2.5m. The real-time reversing image shown in Figure 3 is set as the input of the MWTCMA simulation system.

Compared with CMA and WTCMA, in this simulation, the equalizer order is set to 17, and the equalizer initial input signal is set to $\boldsymbol{g}(n)=[-0.145,0,0,1,0,0]^{\mathrm{T}}$, $\boldsymbol{R}_2=39320.0$, and $J=2$ [16]. Other parameters are set as shown in Table 1. The simulation results are shown in figure 6. Figure 4 is the restoration results by using the CMA algorithm [20], and Figure 5 shows the restoration results using MTCMA mentioned in literature.

In addition, this paper also takes into account the input images used by three various methods all have interference noise, because they are collected by onboard camera. In order to make the simulation results more comparative, the paper also compares the simulation results with the photo collected by a digital camera at the same angle with the onboard camera. The photo collected in this way hasn't the environment interference.

Table 1. Simulation Settings

Algorithm	simulation Step	wavelet	Decomposition Plies	β	Initialize weights
CMA	0.00043		3		The initial value of the 4th tap is set to 1, and others are set to 0.
WTCMA	0.00178	DB5	3	0.9903	
MWTCMA	0.00223	GHM	3	0.9999	

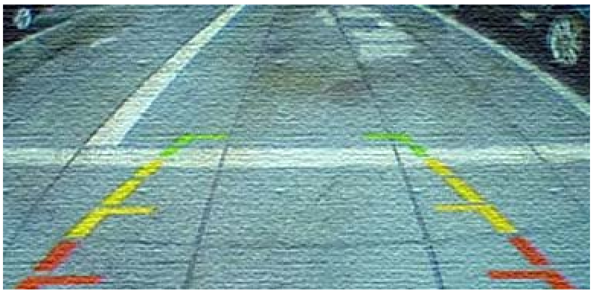

Figure 3. Original input image

Figure 4. Output of CMA algorithm

Figure 5. Output of WTCMA algorithm

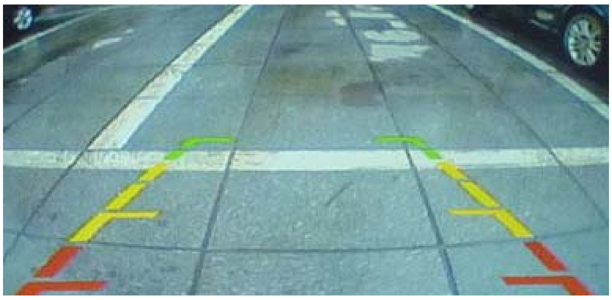

Figure 6. Output of MWTCMA algorithm

Figure 7. Digital camera photo

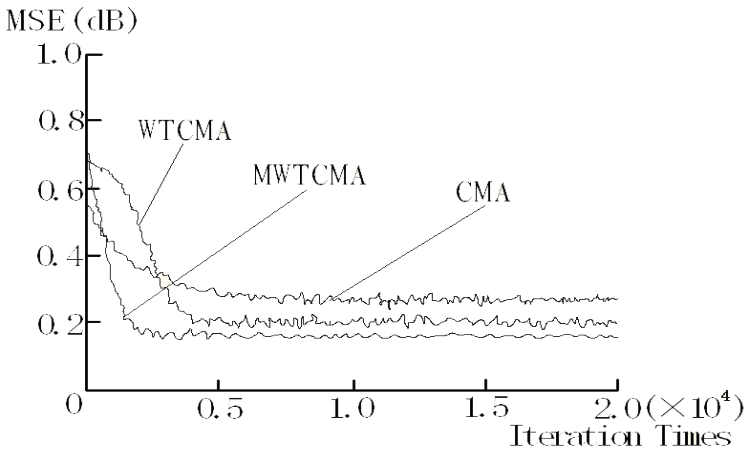

Figure 8. MSE convergence curves of three different algorithms

5. Results and Discussion

Figure 4 to Figure 6 show the restoration effect of various algorithms. Figure 8 shows the MSE convergence curves of three different algorithms. From those figures, we can see that the influences of noise are clearest in CMA among the three algorithms. The restoration effect of CMA is poorest, and its computational amount also is the largest of the three algorithms. Using the image signal statistical information, MWTCMA and WTCMA are least influenced by simulation initial values, and the effect of their restoration is relatively similar to each other. Compared with CMA, MWTCMA and WTCMA also have the better robustness to noise. Simultaneously operating with matrix, MWTCMA and WTCMA also decrease the computational complexity, and improve the restoration effect. In three simulation results shown in those figures, MWTCMA is the clearest one. And compared to the digital camera photo, as shown in figure 7, MWTCMA output image is also the most closest to realistic images among the three simulation output images.

Figure 8 shows that the convergence speed is faster than CMA for approximate 5500 steps, and faster than WTCMA for about 2200 steps. In the steady-state error, MSE of MWTCMA is smaller than CMA for 0.1dB, and is smaller than WTCMA for about 0.05dB.

Table 2. Performance comparison of three various algorithms

Algorithm	CMA	WTCMA	MWTCMA
PSNR	23.912	24.231	26.575
Time/s	13.117	8.014	5.824

Table 2 shows the car reversing image, transmitted by information bus, restoration time consumption of the three different algorithms, CMA, WTCMA and MWTCMA, simulated by the same computer with 1.60GHz CPU and 1GB ROM. MWTCMA, the proposed algorithm by this paper, improves operating efficiency, because it can avoid the high dimensional image matrix inverse operation and the repeatedly alternating iteration process. So, MWTCMA still has certain advantages on amount of computation, which is more conducive for real-time implementation.

Table 2 also gives peak signal to noise ratio (PSNR, characterizes the approximation degree of a restored image on the original image.) of the three different blind restoration algorithms. The higher the PSNR is, the better it restores, and the closer to the original image. PSNR can be defined as:

$$PSNR = 10\lg \frac{255^2}{\frac{1}{N^2}\sum_{i=0}^{N-1}\sum_{j=0}^{N-1}[f_{ij} - \hat{f}_{ij}]^2} \tag{7}$$

Seen from Table 2, due to the presence of the image matrix operation and the iterative calculation of the inverse matrix, WTCMA increases the amount of computation. Increasing the complexity of the algorithm design and the complexity of the algorithm, CMA is constrained by the initial value significantly, which is not conducive to guarantee algorithm stability. And CMA is also easily affected by noise, which is not conducive to real-time implementation. Since the introduction of GHM multi-wavelet transform, MWTCMA reduces the time consumption, ameliorates the quality of restoration, and improves the convergence performance. So MWTCMA has the best balance in PSNR and computational complexity.

6. Conclusion

Charactering with orthogonality, 2-order vanish moment, symmetry and finite supporting, balanced GHM multi-wavelet is used in this paper to restore car reversing image, which is transmitted by information bus. The results show that, MWTCMA has faster convergence speed and higher computational efficiency, and the algorithm is more effective for real-time image signal restoration. MWTCMA can satisfy the requirements of modern car information bus scheduling better. But the multi-wavelet can still be selected manually by using the method of experiment at present.

Acknowledgments

This work was financially supported by the Scientific Research Project of Education Department of Zhejiang Province, P.R. China (Y201329952). And it was also supported by Humanities and Social Science Planning Fund of Ministry of Education of P.R. China (12YJAZH224), the 2013 Annual Research Project of China Society of Logistics (2013CSLKT133), 2012-2013 China Institute of Vocational Education Research Planning Project (570824).

References

[1] Zhang Xinfeng, Yang Diange, Lu Liang. Dynamic Scheduling Algorithm for Local Interconnect Network and Its Application. *Transactions of the Chinese Society of Agricultural Machinery*. 2009; 40(3): 21-25.
[2] Zhuangwen Wu. Analysis Vehicle TWC Light-off Characteristics on AMESim Platform. *TELKOMNIKA Indonesian Journal of Electrical Engineering*. 2013; 11(2): 1076-1082.
[3] Miucic R, Mahmud SM, Popovic Z. An Enhanced Data-Reduction Algorithm for Event-Triggered Networks. *IEEE Transactions on Vehicular Technology*. 2009; 58(6): 2663-2678.
[4] YAN Nan-ming, ZHANG Yu-nan, WANG He-yuan. Design of New Control System in Electric Drive Vehicle. *ACTA ARMAMENTARII*. 2012; 33(2): 232-236.
[5] Yun Seok Choi, Kyun Hyon Tchah. Discrete multi-wavelet transformed adaptive equalizer. *Electronics Letters*. 2002; 38(25): 1745-1747.
[6] Yu Linan, Piao Yan, Yan Xiaoyuan. Video Defogging Based on Adaptive Tolerance. *TELKOMNIKA Indonesian Journal of Electrical Engineering*. 2012; 10(7): 1644-1654.
[7] Goupil A, Palicot J. New Algorithms for Blind Equalization: The Constant Norm Algorithm Family. *IEEE Transactions on Signal Processing*. 2007; 55(4): 1436-1444.
[8] Goossens B, Pizurica A, Philips W. Image Denoising Using Mixtures of Projected Gaussian Scale Mixtures. *IEEE Transactions on Image Processing*. 2009; 18(8):1689-1702.
[9] Ho S, Hong. Scheduling algorithm of data sampling times in the integrated communication and control systems. *IEEE Transactions on Control Systems Technology*. 1995; 3(2):225-230.
[10] Hong SH, Kim WH. Bandwidth allocation scheme in CAN Protocol, Control Theory and Applications. *IEE Proceedings*. 2000; 147(1): 37-44.
[11] Almeida L, Pedreiras P, Fonseca JAG. The FTT-CAN Protocol: why and how. *Industrial Electronics, IEEE Transactions on*. 2002; 49(6):1189-1201.
[12] Pascal Bianchi. Philippe Loubaton. On the Blind Equalization of Continuous Phase Modulated Signals Using the Constant Modulus Criterion. *IEEE Transactions on Signal Processing*. 2007; 55(3): 1047-1061.
[13] Nolte T, Nolin M, Hansson HA. Real-time server-based communication with CAN. *IEEE Transactions on Industrial Informatics.* 2005; l(3): 192-201.
[14] Afonso MV, Bioucas-Dias JM, Figueiredo MAT. Fast Image Recovery Using Variable Splitting and Constrained Optimization. *IEEE Transactions on Image Processing*. 2010; 19(9): 2345-2356.
[15] Johnson BR. Multi-wavelet moments and projection pre-filters. *IEEE Trans on Signal Process.* 2000; 48(11): 3100-3108.
[16] Fowler JE, Li Hua. Wavelet transforms for vector fields using omni directionally balanced multi-wavelets. *IEEE Transactions on Signal Processing*. 2002; 50(10): 3018-3027.
[17] Kreutz-Delgado K, Isukapalli Y. Use of the Newton Method for Blind Adaptive Equalization Based on the Constant Modulus. *IEEE Transactions on Algorithm Signal Processing*. 2008; 56(8): 3983-3995.
[18] LAM EY. Blind bi-level image restoration with iterated quadratic programming. *IEEE Transactions on circuits and systems-II: Express briefs*. 2007; 54(1): 52-56.
[19] VURAL C, SETHARES W A. Blind image deconvolution via dispersion minimization. *Digital Signal Processing*. 2006; 26(3): 137-148.
[20] Saeed Masaebi, Amir Masoud Eftekhary Moghaddam. A New Approach for Image Hiding Based On Contourlet Transform. *International Journal of Electrical and Computer Engineering.* 2012; 2(5): 663-671.